JNCI Cancer Spectrum (2019) 2(3): pky043

doi: 10.1093/jncics/pky043
Article

ARTICLE

Skeletal Muscle Fibrosis in Pancreatic Cancer Patients with Respect to Survival

Sarah M. Judge, Rachel L. Nosacka, Daniel Delitto, Michael H. Gerber, Miles E. Cameron, Jose G. Trevino, Andrew R. Judge

See the Notes section for the full list of authors' affiliations.
Correspondence to: Sarah M. Judge, PhD, Department of Physical Therapy, University of Florida College of Public Health and Health Professions, HPNP Bldg Rm 1142, 1225 Center Dr, Gainesville, FL 32610 (e-mail: smsenf@ufl.edu); or Andrew R. Judge, PhD, Department of Physical Therapy, University of Florida College of Public Health and Health Professions, HPNP Bldg Rm 1142, 100 Center Dr, Gainesville, FL 32610 (e-mail: arjudge@phhp.ufl.edu).

Abstract

Background: Cancer cachexia is a catabolic condition characterized by skeletal muscle wasting, consequent to tumor burden, which negatively impacts tolerance to cancer therapies and contributes to increased mortality. Partly because of the limited knowledge of the underlying mechanisms of cancer cachexia derived from human studies, however, the ability to therapeutically intervene remains elusive. The purpose of the current study was therefore to better define the phenotype of skeletal muscle obtained from patients with pancreatic ductal adenocarcinoma (PDAC), which has one of the highest rates of cachexia.
Methods: Morphological analyses were performed on rectus abdominis muscle biopsies obtained from resectable PDAC patients undergoing tumor resection surgery (N = 20) and from weight-stable non-cancer control subjects undergoing benign abdominal surgery (N = 16). PDAC patients with a body weight loss of greater than 5% during the previous 6 months were considered cachectic (N = 15). Statistical tests were two sided.
Results: Skeletal muscle from cachectic PDAC patients had increased collagen content compared with non-cancer control subjects (1.43% vs 9.66%, $P = .0004$, Dunn test). Across all PDAC patients, collagen content positively correlated with body weight loss ($P = .0016$, $r = 0.672$), was increased in patients with lymph node metastasis ($P = .007$, Mann-Whitney U test), and was associated with survival on univariate (HR = 1.08, 95% confidence interval [CI] = 1.02 to 1.04, $P = .008$) and multivariable analyses (HR = 1.08, 95% CI = 1.00 to 1.17, $P = .038$). Cachectic PDAC patients also displayed increased lipid deposition (2.63% vs 5.72%, $P = .042$), infiltration of CD68+ macrophages (63.6 cells/mm^2 vs 233.8 cells/mm^2, $P = .0238$), calcium deposition (0.21% vs 2.51%, $P = .030$), and evidence of deficient cellular quality control mechanisms (Mann-Whitney U test). Transcriptional profiling of all patients supported these findings by identifying gene clusters related to wounding, inflammation, and cellular response to TGF-β upregulated in cachectic PDAC patients compared with non-cancer control subjects.
Conclusions: To our knowledge, this work is the first to demonstrate increased collagen content in cachectic PDAC patients that is associated with poor survival.

Cachexia is a complex, devastating effect of cancer that is characterized by profound and ongoing loss of skeletal muscle, with or without the loss of fat, that leads to progressive functional impairment and that cannot be fully reversed through nutritional support (1). In general cancer cachexia is a multifactorial syndrome that encompasses metabolic disruptions, hormonal abnormalities, and inflammation leading to negative energy balance and breakdown of muscle and adipose tissue (1). Cachexia may be a consequence of secretions from tumor cells and/or host cells, insulin resistance, anorexia, and cancer therapies (including chemotherapy and radiation) (2). Cachexia negatively impacts both quality of life and tolerance to cancer

Received: May 2, 2018; **Revised:** June 20, 2018; **Accepted:** July 25, 2018

therapies (1–4) and is associated with poor outcomes and decreased survival (5–7). Cachexia most commonly afflicts patients with cancers of the gastrointestinal tract, lung, prostate, and pancreas, with pancreatic ductal adenocarcinoma (PDAC) among those with the highest indices of cachexia. Indeed, a recent study showed cachexia was present in 63% of newly diagnosed PDAC patients (6), which increases up to 80% as the disease progresses (8).

Currently the only potential cure for pancreatic cancer and its associated cachexia is complete surgical resection of the tumor. However, this is possible only in non-metastatic and locally restricted stages, of which only 15% to 20% of patients are eligible at first presentation (9,10). Of those who do undergo tumor resection, only 70% have tumors that are fully resectable during the surgery, and the prognosis for all remains poor due to the high rate of local recurrence and/or distant metastasis (11). Thus, for the vast majority of PDAC patients, treatments are targeted toward extending survival and increasing quality of life, both of which are directly related to cachexia. In fact, studies in tumor-bearing mice have demonstrated that treatments that prevent muscle loss can prolong survival even if they have no effects on tumor growth (12,13). Therefore, developing countermeasures that deter muscle wasting in response to cancer could lead to major advances in improving the quality of life and extending survival in a majority of PDAC patients.

A major constraint in the development of muscle-preserving clinical therapies is the limited knowledge of the underlying mechanisms of cachexia derived from human studies. This is likely due, at least in part, to the challenges of obtaining tissue samples from an increasingly fragile population. Experimental models of cancer cachexia indicate that skeletal muscles undergo fiber atrophy, but no other overt morphological changes, and that the fiber atrophy is broadly due to altered protein and energy metabolism via disruptions to the protein synthesis/degradation and energy production/expenditure balances (14). For more detail of these mechanisms in tumor-bearing mice, the reader is referred to two recent reviews (4,15). Although these preclinical mechanistic studies are critically important, thus far only one drug developed from such studies (Anamorelin, a ghrelin receptor agonist) has improved cachexia symptoms in phase 3 trials (16). To move the field forward toward developing more effective therapies targeting cachexia in cancer patients, it is essential to better define the cachectic phenotype of skeletal muscle in response to human cancer, which was the purpose of the current study.

Methods

For complete detailed methods (including histological staining protocols, antibodies, and quantitative reverse transcriptase polymerase chain reaction [qRT-PCR] primers), see Supplementary Methods (available online).

Patient Population and Skeletal Muscle Biopsies

Skeletal muscle biopsies from the rectus abdominis muscle were obtained from eligible patients following a prospective collection model. Separate portions of each muscle specimen were embedded in optical coherence tomography (OCT) and frozen in isopentane cooled in liquid nitrogen (for histology) or immediately flash frozen in liquid nitrogen (for RNA isolation). Muscle specimens from a subset of patients were also fixed and processed for ultrastructural analysis.

The eligible population consisted of confirmed PDAC patients undergoing surgical resection with curative intent at the University of Florida Pancreatic Surgical Center, or weight-stable patients undergoing benign abdominal surgery, as appropriate non-cancer control subjects, between March 2015 and September 2017. The study was approved by the University of Florida Institutional Review Board and written informed consent was obtained from all participants. All biopsies were obtained at the beginning of the operation from $n = 20$ PDAC patients and $n = 16$ weight-stable non-cancer control subjects. Based on the diagnostic criteria set forth by a panel of experts in cancer cachexia (1), PDAC patients with a body weight (BW) loss of greater than 5% during the previous 6 months were considered cachectic. According to this criteria, $N = 15$ PDAC patients were cachectic and $N = 5$ PDAC patients were non-cachectic. We did not consider patient body mass index (BMI) as an indicator of cachexia because recent work shows that cancer patients with a large BMI may have low muscle mass (17). BW loss and BMI were calculated from BW and height measurements obtained from electronic medical records.

Muscle Histology and Imaging

Serial skeletal muscle sections (10 μM) were cut and transferred to positively charged glass slides. Morphology was evaluated in muscle sections from all patients using hematoxylin and eosin (H&E), Masson's Trichrome (stains collagen) and Oil Red O (stains lipid). A subset of cachectic PDAC patients and non-cancer control subjects were further processed using Alizarin Red S (stains calcium), CD68 antibody (to label macrophages) and antibodies against UBIQUITIN, P62, LAMP1 and LC3 to assess pathways involved in cellular quality control. All images were obtained using a Leica DM5000B microscope (Leica Microsystems; Bannockburn, IL) and analyzed using ImageJ software. Detailed methods have been described by us previously (18) and can be found in Supplementary Methods (available online).

RNA Isolation, Microarray and qRT-PCR

Total RNA was isolated as performed and described previously following homogenization in TRIzol (19). Microarray analysis was performed by the Boston University Microarray and Sequencing Resource Core facility as described previously (20) on RNA samples from 36 patients ($n = 16$ non-cancer control subjects, $n = 15$ cachectic PDAC patients, and $n = 5$ non-cachectic PDAC patients). Differential gene expression analyses were performed using Gene Pattern ($1.20 > fc < -1.20$, $P < .05$) and gene sets analyzed using the DAVID Bioinformatics database (21,22), version 6.8 as detailed in Supplementary Methods (available online). Select genes of interest were validated via qRT-PCR using Applied Biosystems PCR system and TaqMan Gene Expression Assays.

Statistical Analysis

All statistical analyses were performed using GraphPad Prism version 7 (GraphPad Software, San Diego, CA) and SPSS version 22.0 statistical software package (IBM SPSS statistics for Windows; IBM Corp, Armonk, NY). Continuous variables were analyzed using Mann-Whitney U test to compare two groups,

Kruskal-Wallis test to compare groups of at least three and Dunn multiple comparisons post-hoc test, when necessary. Univarate correlations were performed between continuous variables using Spearman rank-order correlation coefficient. For PDAC patients, Kaplan-Meier survival curves were generated for percent area occupied by collagen, using less than and greater than 10% collagen as the cutoff for dichotomization, and for N0- vs N1-stage patients, and evaluated using the log-rank (or Mantel-Cox) test. The effects of continuous variables on survival were evaluated using a Cox proportional hazards model. The assumption of proportionality was confirmed using time-dependent covariates as well as visual inspection of log-log plots. Variables that showed associations with survival on univariable analysis were incorporated into multivariable analysis. All tests were two-sided, and statistical significance was established at P less than .05.

Results

Because the focus of the current study was cachexia, defined as greater than 5% BW loss during the previous 6 months, we compared percent BW loss across patient demographics and clinicopathological parameters available to us for this study (Table 1). Across PDAC patients there were no statistically significant differences in percent BW loss based on sex, tumor size, neoadjuvant therapy, tumor differentiation, N stage or lymphovascular invasion. Mean age was also not different between non-cachectic and cachectic PDAC patients and age did not correlate with percent BW loss ($P = 0.7830$, $r = 0.068$).

Increased Collagen Deposition in Cachectic PDAC Patients, BW Loss, and Decreased Survival

To assess gross skeletal muscle morphology, skeletal muscle sections from PDAC patients and non-cancer control subjects were stained with H&E (Figure 1). Compared with non-cancer control subjects and non-cachectic PDAC patients, cachectic PDAC patients displayed evidence of skeletal muscle pathology characterized by centralized nuclei, abnormal myofiber membranes and fiber damage, increased numbers of mononuclear cells, and increased connective tissue surrounding myofibers.

We further processed muscle sections using Masson's Trichrome staining to identify collagen deposition (fibrotic tissue) (Figure 2, A–C). The percent area occupied by collagen was increased in skeletal muscle from cachectic (but not non-cachectic) PDAC patients compared with non-cancer control subjects (9.66% vs 1.43%, $P = .0004$) (Figure 2D, Table 1), and across all PDAC patients was positively correlated with percent BW loss ($P = .0016$, $r = 0.672$) (Figure 2E). Collagen content did not correlate with age ($P = .909$, $r = 0.028$), BMI ($P = .318$, $r = -0.242$), or tumor size ($P = .323$, $r = 0.2398$) (graphs not shown) and was not different between males and females (Table 1). We also found no differences in collagen content following stratification of PDAC patients based on neoadjuvant therapy, tumor differentiation, disease stage, or lymphovascular invasion (Table 1). We did, however, find greater collagen content in PDAC patients with (N1, 11.47%), vs no (N0, 2.27%), regional lymph node metastasis ($P = .007$) (Figure 3A, Table 1). Because lymph node metastasis is known to be associated with poor survival (23), we further performed Kaplan-Meier analyses on PDAC patients dichotomized by either N stage or collagen content less than and greater than 10%. Both the absence of regional lymph node metastasis ($P = .0073$, Figure 3B) and collagen content below 10% ($P = .0047$, Figure 3C) were statistically significantly associated with improved long-term survival. Indeed, PDAC patients surviving more than one year post-surgery had lower collagen deposition compared with patients surviving less than one year post-surgery (3.17% vs 12.22%, $P = .0076$, Figure 3D).

A Cox proportional hazards model was used to evaluate relationships between collagen content within skeletal muscle, clinicopathologic variables, and overall survival after pancreatic resection with curative intent (Figure 3E). Univariate analysis confirmed known correlations between positive surgical margin, lymphatic metastasis, and poor survival. Interestingly, high skeletal muscle collagen content was similarly associated with poor survival (HR = 1.08, 95% CI = 1.02 to 1.04, $P = .008$). Multivariable analysis further confirmed the statistical significance of increased collagen content in predicting overall survival (HR = 1.08, 95% CI = 1.00 to 1.17, $P = .038$), demonstrating for the first time a statistically significant relationship between intramuscular collagen content and oncologic outcomes in pancreatic cancer.

Because the replacement of muscle tissue with fibrotic tissue is commonly associated with fat deposition, we also processed muscle sections using Oil Red O staining, which stains lipid (Figure 4, A and B). Compared with non-cancer control subjects, we identified an increase in lipid deposition in cachectic (2.63% vs 5.72%, $P = .042$), but not non-cachectic (2.63% vs 3.29%, $P \geq .999$) PDAC patients (Figure 4C), much of which was localized to areas of muscle fibrosis. Correlative analysis between fat content and percent BW loss, however, was not statistically significant ($P = .135$, $r = 0.326$). Since the pathological development of both adipogenesis and fibrosis in skeletal muscle is known to be associated with the expansion and differentiation of fibro/adipogenic progenitor (FAP) cells that are positive for platelet-derived growth factor receptor alpha (PDGFRα) (24), we further stained muscle sections from a subset of non-cancer control subjects and cachectic PDAC patients using an antibody against PDGFRα. As shown in Figure 4D, PDGFRα-positive FAP cells were visually more abundant in muscle of cachectic PDAC patients compared with non-cancer control subjects, and were localized near areas of connective tissue deposition (Supplementary Figure 1, available online).

Muscle Fibrosis in Cachectic PDAC Patients and Muscle Damage, Calcium Deposition, and Macrophage Infiltration

Based on our novel finding of fibrosis in cachectic PDAC patients, we further evaluated a subset of cachectic PDAC patients (and a subset of age-matched and sex-matched non-cancer control subjects) for additional pathologies commonly associated with the development and progression of fibrosis, including muscle damage, calcium deposition, and macrophage infiltration (25,26). Muscle fiber architecture was assessed at the ultrastructural level using transmission electron microscopy (TEM), which revealed considerable evidence of ultrastructural myofiber damage in cachectic PDAC patients, including disruptions to the myofiber membrane and myofiber fragmentation (Figure 5, A–C). Staining of muscle sections with Alizarin Red S or CD68 antibody revealed an increase in the percent of muscle area positive for calcium deposition (Figure 5, D–L, 0.21% vs 2.51%, $P = .0238$) and an increase in the number of CD68+ macrophages (Figure 5, M–O, Q, 63.6 cells/mm^2 vs 233.8 cells/mm^2, $P = .0303$) in cachectic PDAC patients compared with non-cancer control subjects.

Table 1. Patient demographics

Variable	Number or mean (SEM)	*P*	% BW loss (95% CI)	*P*	% Collagen content (95% CI)†	*P*
Condition						
Non-cancer control subjects	16		−0.88 (−2.92 to 1.14)	<.0001*	1.43 (1.09 to 1.76)	.0009*
PDAC	20		12.34 (8.21 to 16.47)		8.08 (3.84 to 12.32)	
Non-Cachectic PDAC	5		1.98 (−0.61 to 4.57)	<.0001*	2.16 (−1.15 to 5.48)	.011*
Cachectic PDAC	15		15.79 (11.74 to 19.85)		9.66 (4.52 to 14.79)	
Sex						
Non-cancer control subjects						
Male	5		−0.22 (−2.73 to 2.29)	.97	1.64 (0.32 to 2.96)	.913
Female	11		−1.22 (−4.32 to 1.88)		1.33 (1.12 to 1.53)	
PDAC						
Male	10		10.02 (3.04 to 17.00)	.18	7.69 (−0.69 to 16.07)	.865
Female	10		15.87 (9.65 to 22.10)		8.43 (3.43 to 13.42)	
Age, y						
Non-cancer control subjects	57.6 (2.92)	.005*				
PDAC	67.8 (1.96)					
Non-cachectic PDAC	67.2 (2.71)	.66				
Cachectic PDAC	68 (2.5)					
BMI						
Non-cancer control subjects	29.31 (1.31)	.09				
PDAC	27.02 (1.13)					
Neoadjuvant Therapy						
Yes	5		16.24 (3.18 to 29.30)	.16	11.18 (−5.22 to 27.58)	.559
No	15		10.38 (5.44 to 15.32)		6.97 (12.95 to 10.99)	
Tumor size, cm						
<3	11		11.24 (4.80 to 17.68)	.76	9.41 (1.48 to 17.33)	.491
>3	9		12.59 (5.11 to 20.07)		6.60 (2.31 to 10.89)	
AJCC Stage 7th						
IA	1		29.4	.16	6.14	.104
IIA	6		7.12 (0.01 to 14.22)		1.62 (0.58 to 2.66)	
IIB	12		12.75 (6.68 to 18.82)		12.26 (5.84 to 18.68)	
III	1		11.8		2.78	
Tumor Differentiation‡						
Well/moderate	12		8.3 (2.05 to 14.55)	.051	5.40 (1.81 to 8.99)	.36
Poor	7		17.04 (11.16 to 22.93)		8.60 (1.46 to 15.74)	
N Stage						
N0	7		10.3 (0.64 to 19.96)	.6	2.27 (0.48 to 4.05)	.007*
N1	13		12.68 (7.15 to 18.21)		11.47 (5.42 to 17.51)	
Lymphovascular Invasion						
Yes	14		11.25 (−0.65 to 23.15)	.86	3.65 (−0.75 to 8.04)	.058
No	6		12.1 (6.94 to 17.26)		10.12 (4.25 to 15.99)	

*Groups were compared using Mann-Whitney U test to compare two groups and Kruskal-Wallis test to compare groups of three or more. AJCC = American Joint Committee on Cancer; BMI = body mass index; BW = body weight; PDAC = pancreatic ductal adenocarcinoma. Stastically significantly different ($P < .05$).
†One non-cachectic PDAC patient had insufficient tissue sample for analysis of collagen content.
‡One adenosquamous cancer patient excluded from the analysis of tumor differentiation.

Accumulation of Protein Aggregates and Giant Vesicles in Cachectic PDAC Patients

TEM imaging of skeletal muscle also revealed giant single-membrane vesicles in cachectic PDAC patients. These vesicles were filled with undigested material [consistent with lipofuscin granules, ie, aggregates of incompletely degraded proteins and lipids (27,28)] and were localized to the myofiber membrane and directly adjacent to myonuclei (Figure 6, A–F). Several light-density lipid inclusions could be observed in each vesicle, many of which were partially or entirely replaced by darkly stained calcifications (29). We therefore further evaluated, via immunohistochemistry, markers of the autophagy-lysosome system (p62, LAMP1, LC3) and the ubiquitin proteasome pathway (UBIQUITIN), which are both involved in the degradation of cellular proteins and lipids (Figure 6, G–R). Compared with non-cancer control subjects, cachectic PDAC patients showed an increase in the staining intensity of ubiquitinated proteins ($P = .0357$) (Figure 6S) and increases in the size of p62+ aggregates ($P = .0043$) (Figure 6T) and LAMP1+ lysosomes ($P = .0159$) (Figure 6V). No changes were identified for LC3 (Figure 6, X and Y).

Genome-wide Microarray Analyses and Skeletal Muscle Damage, Inflammation, and Fibrotic Changes in Cachectic PDAC Patients

Microarray analysis revealed 527 genes (296 upregulated and 231 downregulated) that were differentially expressed in skeletal muscle of cachectic PDAC patients (N = 15) vs non-cancer control subjects (n = 16) (Supplementary Table 1, available online). Of these 527 genes, two were commonly upregulated and

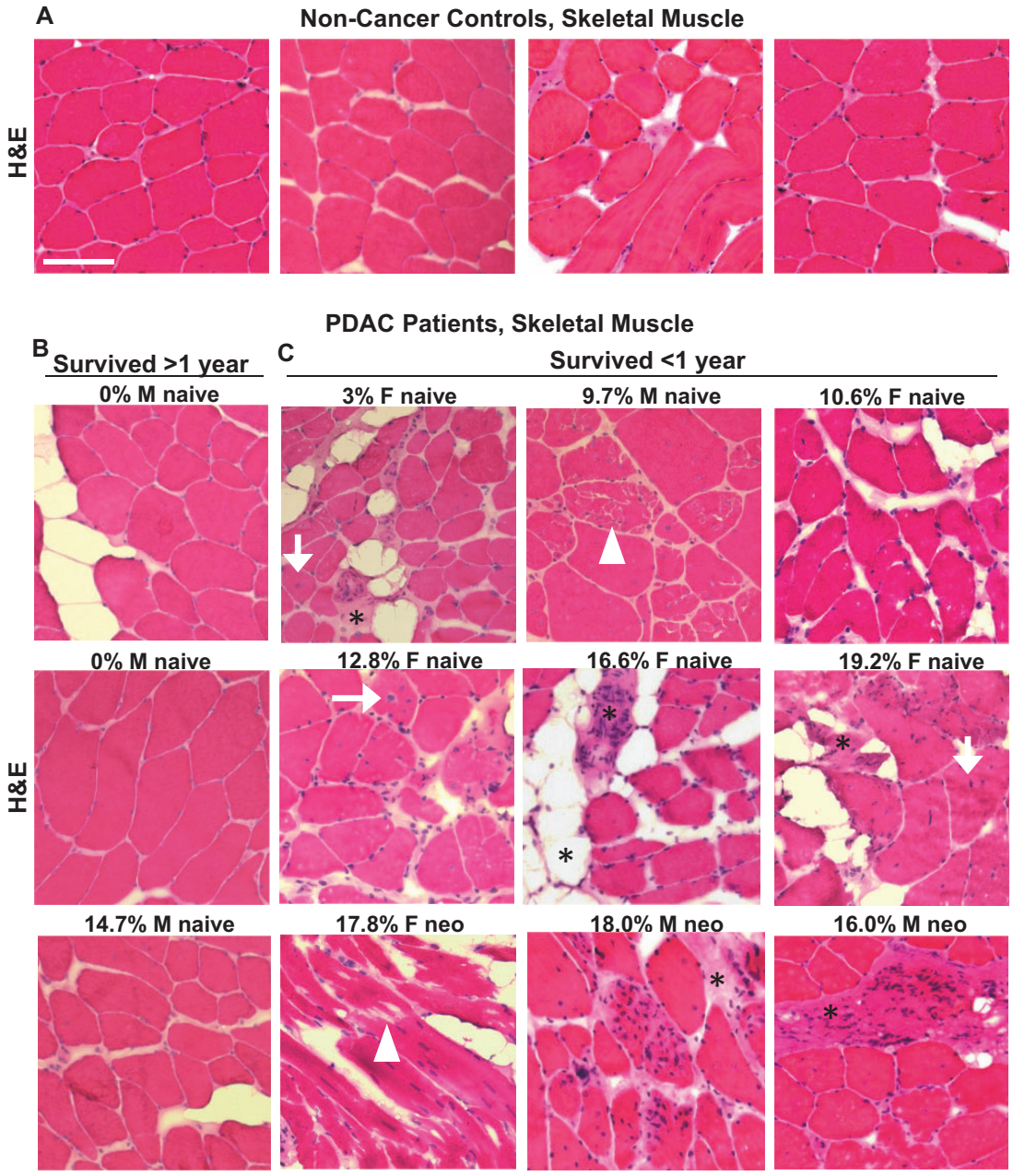

Figure 1. Morphological characteristics of skeletal muscle from non-cancer control patients and PDAC patients. Representative hematoxylin and eosin (H&E) stained sections from the rectus abdominis muscle of weight stable non-cancer control patients **(A)** and PDAC patients **(B, C)** with varying degrees of BW loss (indicated as a percentage) within the 6 months prior to surgery. PDAC patients are further stratified based on survival time of more than 1 year post-surgery **(B)** vs less than 1 year post surgery **(C)**. Morphological features consistent with skeletal muscle pathology are observed in muscle from PDAC patients, including mononuclear cell infiltration, muscle fiber fragmentation (**white arrowheads**), muscle fibers with centralized nuclei (**white arrows**), and connective tissue deposition (*). Images are representative of n = 16 non-cancer control subjects, n = 5 non-cachectic PDAC patients, and n = 15 cachectic PDAC patients. M = male; F = female; neo = received neoadjuvant therapy prior to tumor resection surgery; naïve = naïve to neoadjuvant therapy; PDAC = pancreatic ductal adenocarcinoma. Scale bar = 100 μm.

22 commonly downregulated in non-cachectic PDAC patients vs non-cancer control subjects (Supplementary Table 2, available online). Gene Ontology (GO)/Kegg Pathway analysis of genes upregulated only in cachectic PDAC patients revealed enrichment of multiple GO terms/biological processes that align with our histological findings including "leukocyte activation" ($P = 3.23 \times 10^{-5}$) and "leukocyte migration" ($P = 1.65 \times 10^{-5}$), "response to wounding" ($P = 5.9 \times 10^{-4}$), "fat cell differentiation" ($P = 3.81 \times 10^{-4}$), and "response to transforming growth factor beta (TGF-β)" ($P = 7.55 \times 10^{-4}$), the latter of which is known to be involved in the development of tissue fibrosis. Terms related to pathways previously implicated in cachectic muscle wasting, such as the "FoxO signaling pathway" ($P = .00509$) and "regulation of the MAPK signaling cascade" ($P = 1.99 \times 10^{-6}$), were also enriched. Analysis of genes downregulated only in cachectic PDAC patients identified seven enriched GO terms, all of which were related to "mitochondrion" ($P = 2.51 \times 10^{-7}$), which was the most enriched GO term.

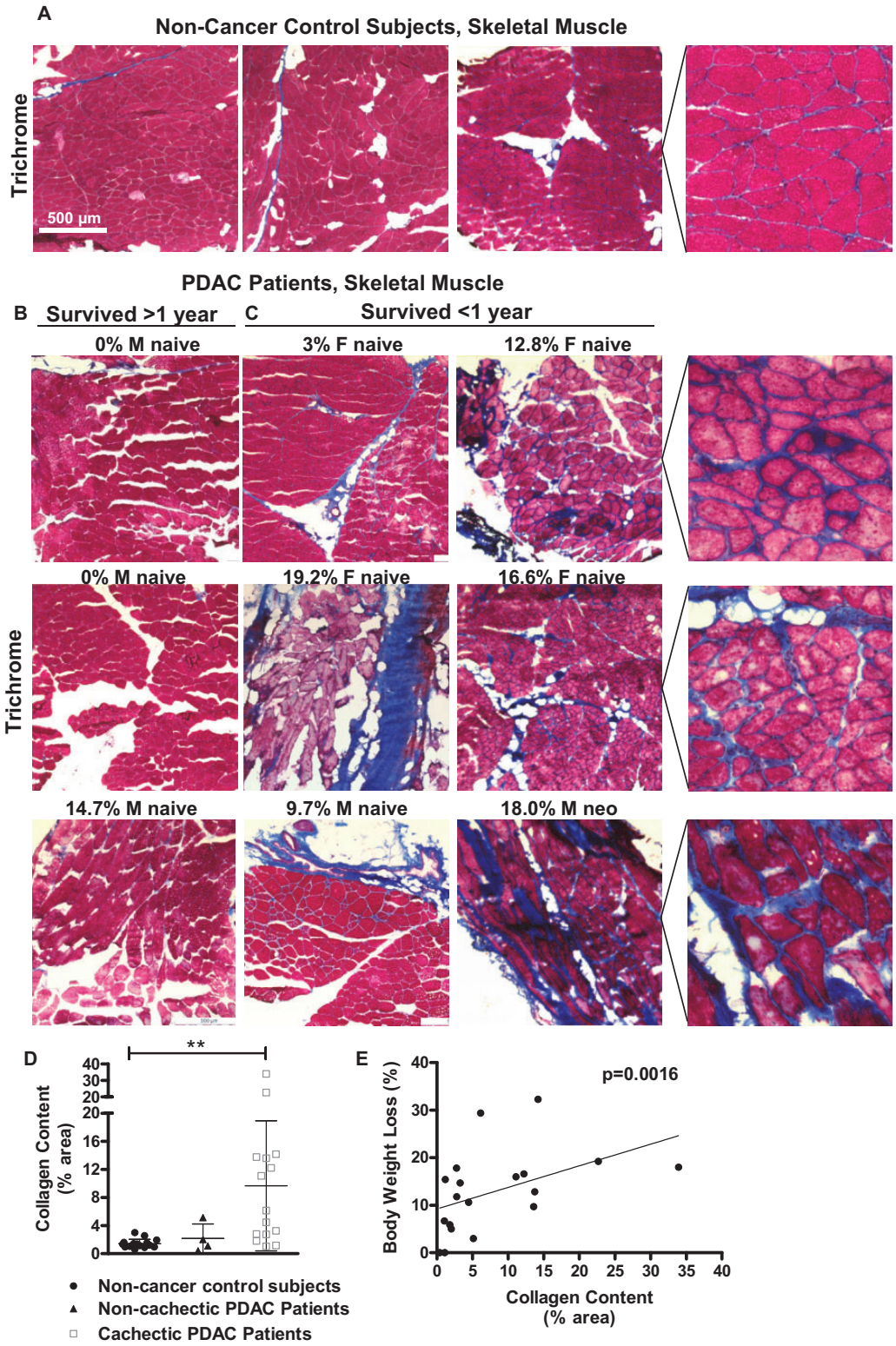

Figure 2. Skeletal muscle collagen content and its relationship with body weight loss in PDAC patients. Representative Masson's Trichrome stained sections (collagen stains blue) from the rectus abdominis muscle of weight stable non-cancer control patients **(A)** and PDAC patients **(B, C)** with varying degrees of BW loss (indicated as a percentage) within the 6 months prior to surgery. PDAC patients are further stratified based on survival time of more than 1 year post surgery **(B)**, vs less than 1 year post surgery **(C)**. Magnified images demonstrate increased staining of collagen (fibrosis) in the endomysium surrounding individual muscle fibers in cachectic PDAC patients. **D)** The percentage of total muscle area (per 5x field) occupied by collagen was quantified in n = 16 non-cancer control subjects, n = 4 non-cachectic PDAC patients (<5% BW loss) and n = 15 cachectic PDAC patients (>5% BW loss) and is expressed as the mean ± SEM (*$P = .0004$, Dunn test). **E)** Relationship between collagen content (% area) and BW loss (%) in PDAC patients (Spearman's correlation, $P = .0016$, $r = 0.672$). BW = body weight; PDAC = pancreatic ductal adenocarcinoma.

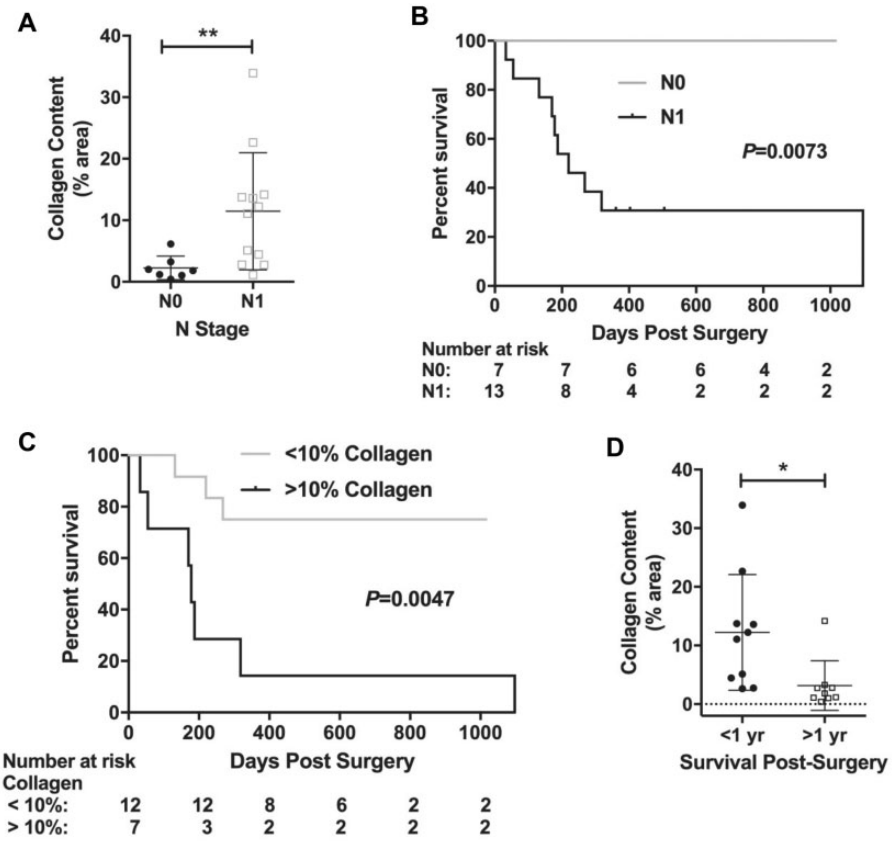

E **Predictors of Survival**

Univariate Analysis	Hazard Ratio	95% Confidence Interval	*P* Value
Age (y)	0.97	0.90 – 1.04	.385
Female Sex	2.28	0.57 – 9.15	.244
Tumor Size (cm)	1.09	0.64 – 1.87	.742
Positive Margin	**4.19**	**1.03 – 17.1**	**.046***
Number of Positive Lymph Nodes	**1.42**	**1.10 – 1.83**	**.008***
Poor Tumor Differentiation	2.72	0.72 – 10.3	.141
Neoadjuvant Therapy	1.78	0.42 – 7.51	.435
Collagen Content	**1.08**	**1.02 – 1.14**	**.008***
Body Weight Loss (lbs)	1.02	0.95 – 1.09	.575
Multivariable Analysis			
Positive Margin	0.93	0.13 – 6.49	.941
Number of Positive Lymph Nodes	**1.43**	**1.01 – 2.03**	**.047***
Collagen Content	**1.08**	**1.004 – 1.17**	**.038***

Figure 3. Relationship between muscle collagen content, lymph node metastasis and survival in PDAC patients. **A)** The percent of total muscle area occupied by collagen in PDAC patients stratified by N stage (N0 vs N1), expressed as mean ± SEM. PDAC patients with positive lymph node metastasis (N1, n = 12) vs PDAC patients with no lymph node metastasis (N0, n = 7) ($P = .0099$, Mann-Whitney U test). **B, C)** Kaplan-Meier analyses on PDAC patients dichotomized by either N stage (**B**, N0 vs N1) or collagen content (**C**, <10%>). **D)** The percent of total muscle area occupied by collagen in PDAC patients surviving >1 year post-surgery vs PDAC patients surviving <1 year post-surgery ($P = .0040$, *Mann-Whitney U test). *Two patients still alive at 10 months and 11 months postsurgery, who had not reached the 1-year mark postsurgery and who had 6.1% and 2.0% collagen content, respectively, were excluded from the analysis. **E)** Univariate analysis was performed using a Cox proportional hazard model. All variables statistically significant ($P < .05$) on univariate analyses were included in multivariable Cox regression.

qRT-PCR Validation and Upregulation of Pro-Fibrotic Genes in Muscle of Cachectic PDAC Patients

Based on our novel finding of skeletal muscle fibrosis in cachectic PDAC patients, we selected to validate in a subset of patients through qRT-PCR the expression of genes related to the TGF-β signaling pathway that were identified via microarray as increased in cachectic PDAC patients compared with non-cancer control subjects. We measured thrombspondin-1 (*THBS1/TSP-1*), which plays a role in fibrosis through its direct activation of latent TGF-β and the TGF-β receptors *TGFBR2* and

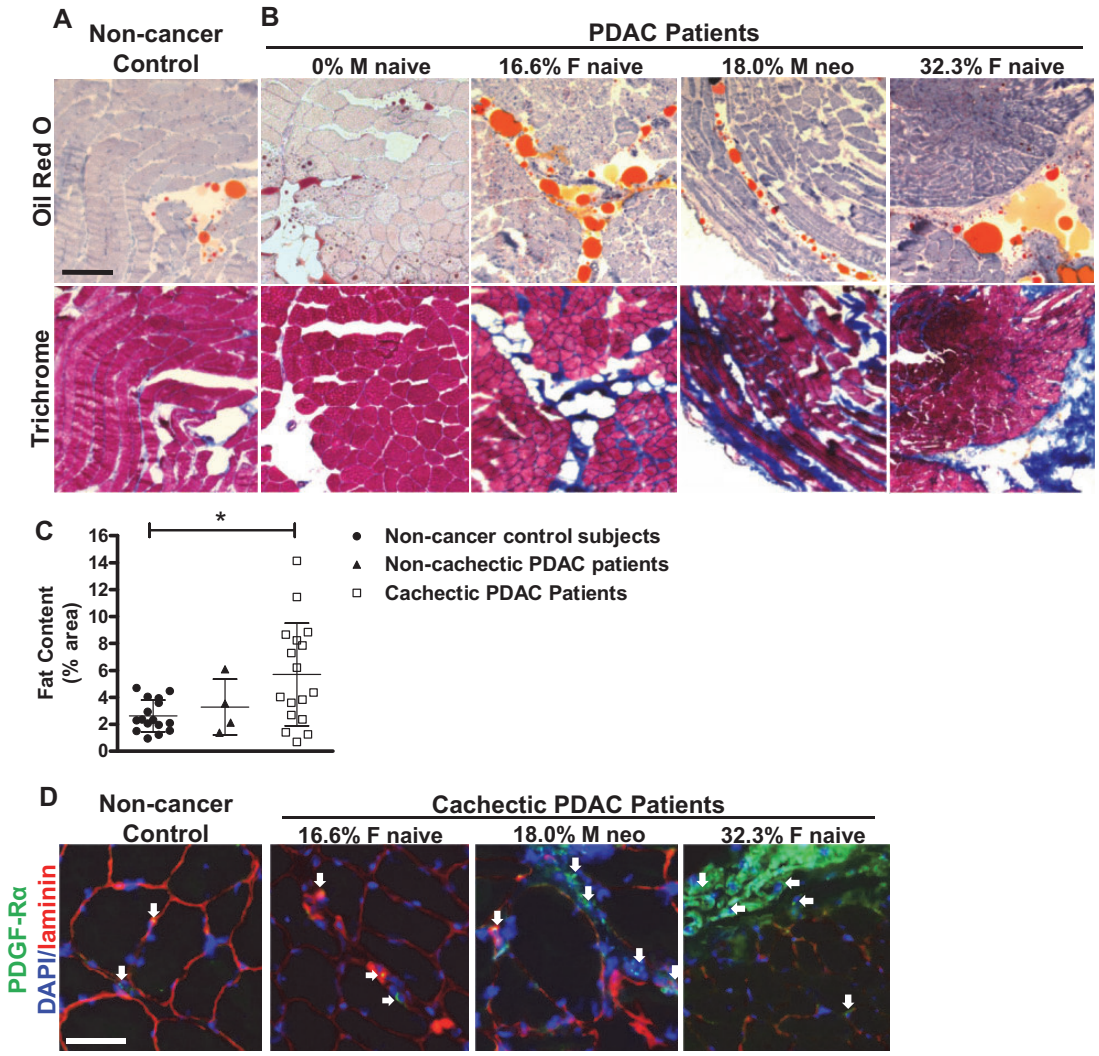

Figure 4. Lipid content in skeletal muscle of non-cachectic and cachectic PDAC patients versus non-cancer control patients. **A, B)** Representative serial sections from the rectus abdominis muscle of non-cancer control patients and PDAC patients with varying levels of BW loss (indicated as a percentage) stained with Oil Red O, which stains lipid orange, or Masson's Trichrome, which stains collagen blue. Scale Bar = 200 μm. **C)** The percent of total muscle area occupied by fat in non-cancer control patients (n = 16), non-cachectic PDAC patients (n = 4) and cachectic PDAC patients (n = 15), expressed as mean ± SEM (*P = .0418, Dunn's test). **D)** Representative skeletal muscle sections from a non-cancer control and cachectic PDAC patients immunostained with antibodies against platelet-derived growth factor receptor alpha (to label fibroadipogenic progenitor [FAP] cells, **green**) and laminin (to label basement membranes, **red**), and counterstained with DAPI (to label cell nuclei, **blue**). Scale bar = 50 μm. **White arrows** = FAP cells. BW = body weight; M = male, F = female, neo = neoadjuvant therapy; naïve = naïve to neoadjuvant therapy; PDAC = pancreatic ductal adenocarcinoma.

TGFBR3/betaglycan. Although TGFBR3 does not participate directly in TGF-β signal transduction, through binding of TGF-β family members it acts as a reservoir of receptor ligands. We also measured connective tissue growth factor (*CTGF/CCN2*) and plasminogen activator inhibitor-1 (*PAI-1/SERPINE1*), both of which are downstream targets of TGF-β that mediate tissue fibrosis. Compared with non-cancer control subjects, cachectic PDAC patients showed increases in *THBS1/TSP-1* (6.9-fold, P = .0491), *TGFBR2* (1.9-fold, P = .0378), *TGFBR3* (2.0-fold, P = .0116), *CTGF* (4.3-fold, P = .0134), and *PAI-1/SERPINE1* (4.9-fold, P = .0062) (Figure 7).

Discussion

To the best of our knowledge, the current findings demonstrate for the first time skeletal muscle remodeling characterized by fibrosis in cachectic PDAC patients. Critically, this study is the first to demonstrate a novel and statisticaly significant relationship between the extent of muscle fibrosis and oncologic outcomes in pancreatic cancer. Indeed, we found that increased collagen content associates with lymph node metastasis and poor survival.

The replacement of muscle tissue with ectopic tissues such as fat and fibrotic tissue is a known consequence of impaired muscle regeneration following muscle damage. Interestingly, evidence of muscle damage, including disruptions to myofiber membranes and increased membrane permeability, are evident in both preclinical models of cancer cachexia (30) and cachectic PDAC patients (31). Furthermore, although satellite cells are activated in cancer cachexia, they are inhibited from completing differentiation and thus muscle regeneration is also impaired (31). Although the underlying causes of muscle damage are not clear, we show here substantial calcium deposition in muscle of

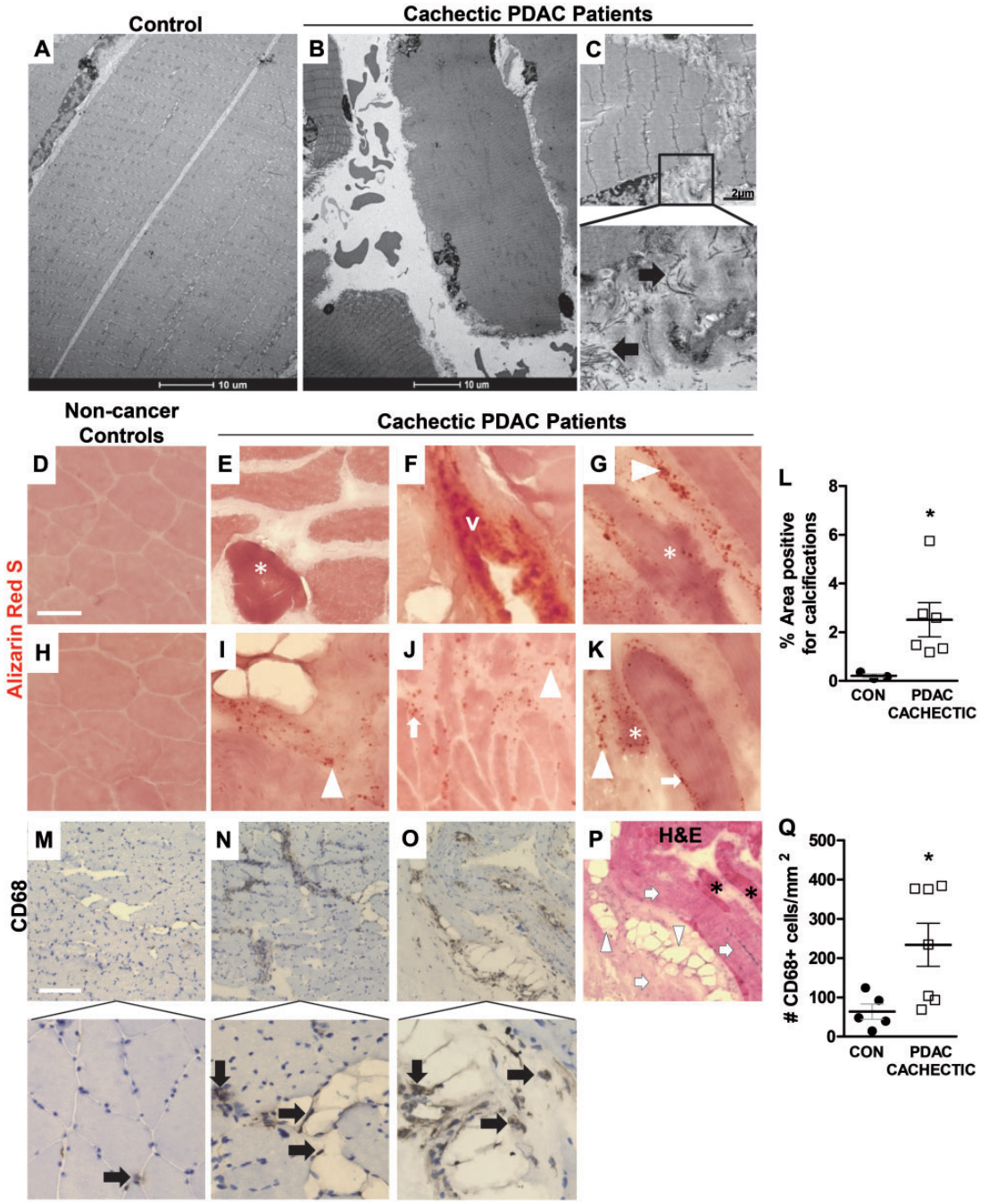

Figure 5. Figure 5. Ultrastructural damage, calcifications and macrophages present in skeletal muscle from cachectic PDAC patients. **A–C)** Representative electron micrographs of skeletal muscle from non-cancer control patients (n = 2) and cachectic PDAC patients (n = 2) following transmission electron microscopy. Areas of ECM deposition are indicated by black arrows. **D–K)** Representative skeletal muscle sections from non-cancer control patients **(D, H)** and cachectic PDAC patients **(E–G, I–K)** stained with Alizarin Red S to label calcium deposition (stains red). Calcium deposits localized inside (*) and at the periphery (white arrows) of muscle fibers, in the extracellular matrix (white arrowheads) and in blood vessels walls (v) are noted. Scale bar: 50 μm. **L)** The percent of total muscle area positive for calcium deposition in non-cancer controls (n = 3) versus cachectic PDAC patients (n = 6), expressed as the mean ± the SEM (P = .0238, Mann-Whitney U test). **M–O)** Representative skeletal muscle sections from a non-cancer control patient **(M)** and cachectic PDAC patients **(M, O)** immunostained with a CD68 antibody to label macrophages (brown staining, black arrows). Scale bar: 200 μm. **P)** Staining of a serial muscle section with H&E to demonstrate the localization of CD68+ macrophages in cachectic muscle. Areas of collagen (light pink staining, white arrows), lipid (white arrowheads) and muscle fibers (black astericks) are indicated. **Q)** The average number of CD68+ macrophages in muscle of cachectic PDAC patients compared to non-cancer control subjects (P = .0303, Mann-Whitney U test). Data represent mean ± SEM, from n = 5 non-cancer controls and n = 7 cachectic PDAC patients. CON = controls; PDAC = pancreatic ductal adenocarcinoma.

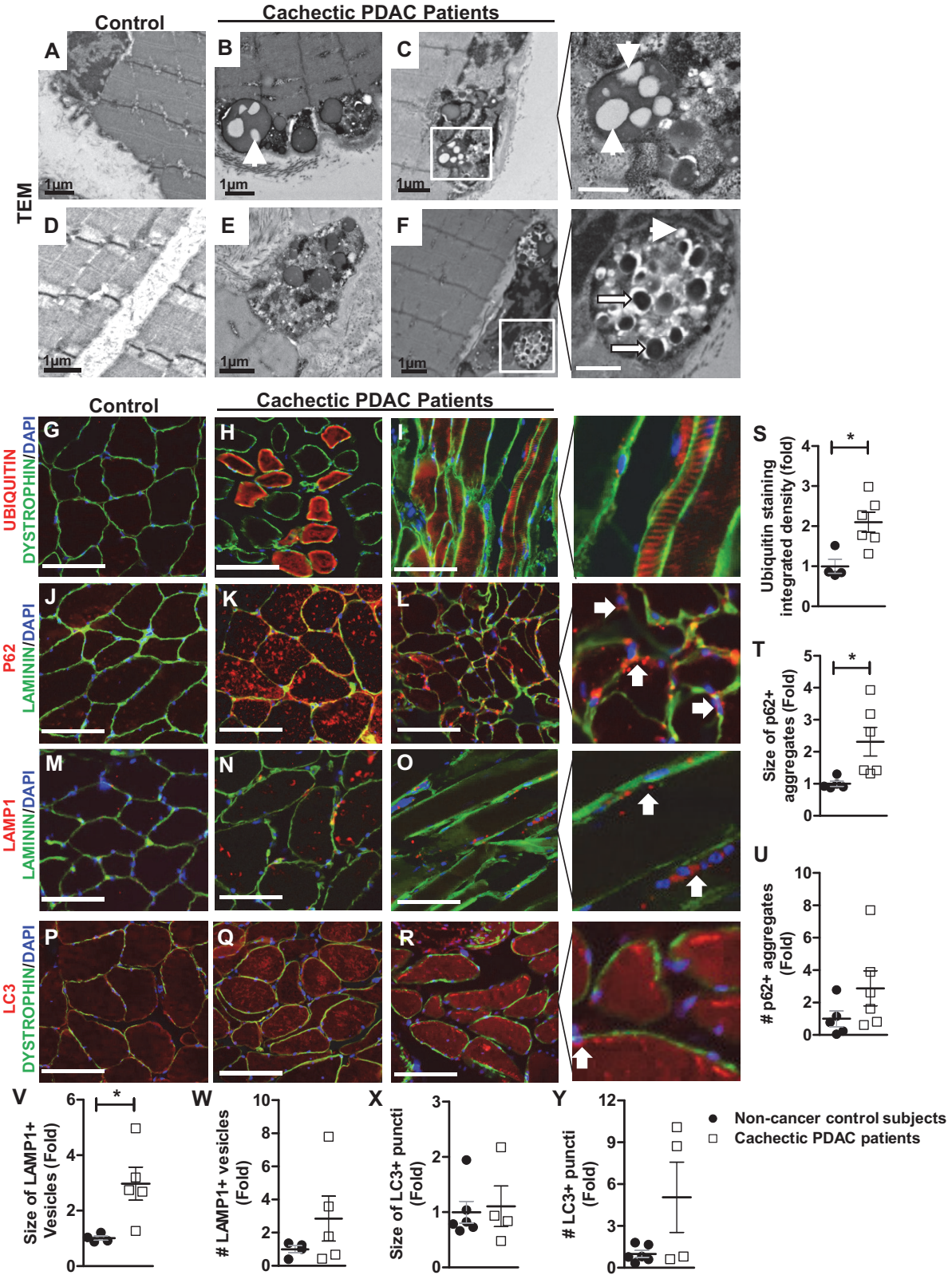

Figure 6. Accumulation of protein aggregates, giant vesicles in skeletal muscle from cachectic PDAC patients. **A–F)** Representative electron micrographs of skeletal muscle from non-cancer control subjects **(A, D)** and cachectic PDAC patients **(B, C, E, F)**. The morphology of these vesicles was consistent with that of autolysosomes containing lipofuscin granules (ie, aggregates of incompletely degraded proteins and lipids). Many of the light-density lipid inclusions (**white arrowheads**) present in the vesicles were partially or entirely replaced by darkly stained calcifications (**long white arrows**), which can be observed more clearly in magnified images. White scale bars = 500 nm. **G–R)** Representative muscle sections from non-cancer control subjects or cachectic PDAC patients stained with antibodies against UBIQUITIN **(G–I)**, p62 **(J–L)**, LAMP1 **(M–O)**, or LC3 **(P–R)** (**red staining**) plus antibodies against either dystrophin or laminin to label fiber membranes (**green staining**) and counterstained

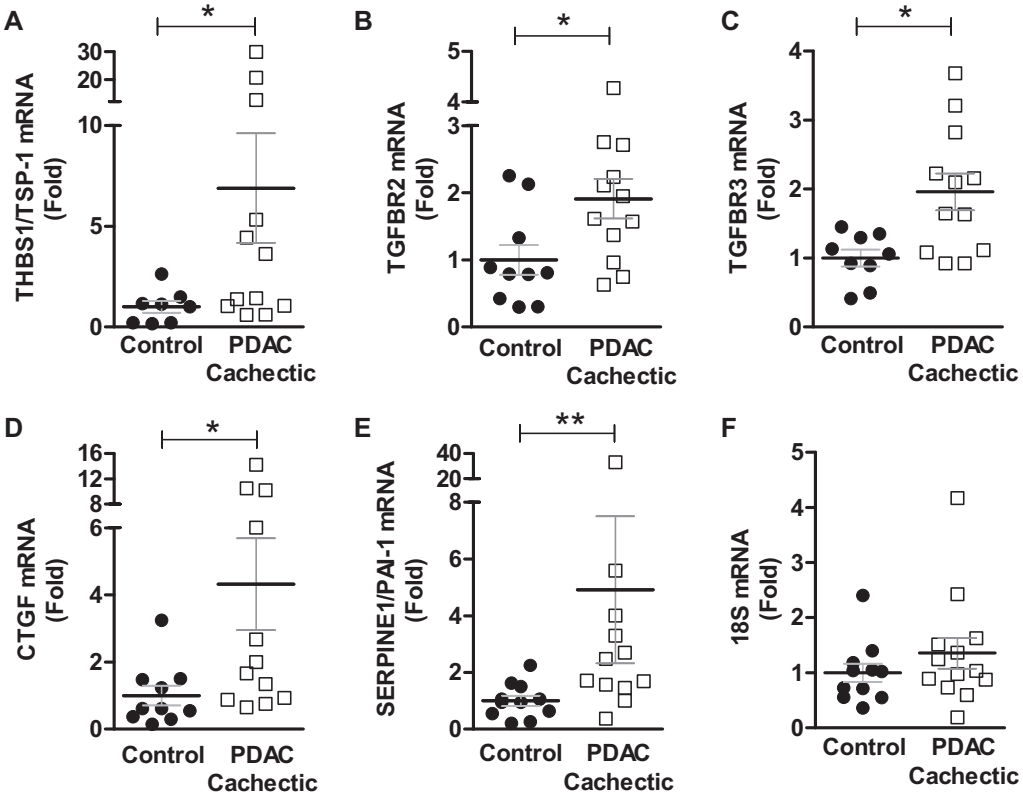

Figure 7. Gene expression of pro-fibrotic factors in skeletal muscle from control and cachectic PDAC patients. Rectus abdominis muscle biopsies from non-cancer control subjects and cachectic PDAC patients were processed for qRT-PCR analyses to validate select genes identified via microarray as increased in cachectic PDAC patients. Compared with non-cancer control subjects, cachectic PDAC patients showed increased gene expression of thrombospondin-1 (THBS1/TSP-1, 6.9-fold, $P = .0491$) **(A)**, *TGFBR2* (1.9-fold, $P = .0378$) **(B)**, TGFBR3 (2.0-fold, $P = .0116$) **(C)**, connective tissue growth factor (*CTGF*, 4.3-fold, $P = .0134$) **(D)**, and plasminogen activator inhibitor-1 (*PAI-1/SERPINE1*, 4.9-fold, $P = .0062$) **(E, F)** The housekeeping gene, 18S, was not statistically significantly different between non-cancer control subjects and cachectic PDAC patients. All samples were run in triplicate on the same PCR plate and were normalized to the mean of the non-cancer control group. Data are expressed as mean ± SEM, from n = 8-10 non-cancer control subjects and n = 12-13 cachectic PDAC patients. $^{*}P < .05$, $^{**}P < .01$, Mann-Whitney U test. PDAC = pancreatic ductal adenocarcinoma; qRT-PCR = quantitative reverse transcriptase polymerase chain reaction.

cachectic PDAC patients that may contribute to muscle damage. Indeed, calcium overload within myofibers could lead to damage via activation of calpains and subsequent proteolysis of cellular constituents; activation of phospholipase A2 and disruptions to the integrity of the sarcolemma; and calcium overload within mitochondria, which can further induce cellular damage and death (32). In addition, although the replacement of muscle tissue with fat can be a consequence of muscle damage and failed regeneration, lipid accumulation within muscle has also been shown to induce muscle damage and impair regeneration (33), while blocking lipotoxicity prevents muscle wasting in tumor-bearing mice (34). In the current study it is not possible to determine whether the lipid accumulation in PDAC patients is a cause or consequence of muscle damage. Lastly, impaired lysosomal-mediated degradation of cellular constituents, including lipids, could also play a role in muscle damage and myopathy because lysosomal deficiencies are known to induce dystrophic-like changes to skeletal muscle (35,36).

The long-term consequences of chronic muscle damage and impaired regeneration are well established and include non-resolute inflammation, proliferation of FAP cells, and progressive replacement of muscle fibers with both fat and fibrotic tissue (25,26). In the current study we provide novel histological data that support this pathological progression toward the replacement of muscle with fat and fibrotic tissue in human pancreatic cancer cachexia. This pathological progression was supported by transcriptional profiling that identified transcripts involved in inflammation, wound healing, and cellular responses to TGF-β (which is a known regulator of tissue fibrosis) upregulated in muscle from cachectic PDAC patients. In fact, TGF-β is a potent inducer of muscle fibrosis (37,38), is a blood biomarker of cachexia in cancer patients (39), and mediates cachexia in tumor-bearing mice (40). Within the muscle of cachectic PDAC patients we confirmed, via qRT-PCR, elevation of transcripts involved in TGF-β activation (THBS1/TSP-1) and signal transduction (*TGFBR2* and *TGFBR3*), and of TGF-β target genes that mediate tissue fibrosis (*CTGF* and *PAI-1*) (41–43). In fact, CTGF is stimulated by TGF-β from both FAP cells (24) and skeletal muscle cells (44), and its overexpression is sufficient to induce skeletal muscle damage and

Figure 6. Continued
with DAPI to label nuclei (**blue**). Scale bar = 100 μm. Magnified images depict the size of p62+ aggregates and LAMP1+ lysosomes in muscle of cachectic PDAC patients, their localization near the myofiber membrane, and their proximity to myonuclei (**white arrows**). **S–Y)** The average staining intensity of ubiquitin and the average size and number of p62+, LAMP1+, or LC3+ puncta in non-cancer control subjects versus cachectic PDAC patients. All data represent the mean ± SEM, from n = 4-5 non-cancer control patients and n = 5-6 cachectic PDAC patients. $^{*}P < .05$, Mann-Whitney U test. PDAC = pancreatic ductal adenocarcinoma.

fibrosis (45). Moreover, its inhibition, via genetic deletion or antibody targeting, ameliorates muscle fibrosis in a mouse model of Duchenne muscular dystrophy (46). Our finding that *THBS1/TSP-1* is increased in cachectic PDAC patients is similarly intriguing, because THBS1/TSP-1 is a direct upstream activator of latent TGF-β, and is a downstream target of Angiotensin II (Ang II) signaling. Similar to TGF-β, Ang II is also a blood biomarker of cachexia in cancer patients (39) and plays a role in muscle fibrosis (47) and cancer-induced muscle wasting in mice (48,49). Therefore, the muscle damage and progressive fibrosis observed in cachectic cancer patients could be mediated, at least in part, through TGF-β and Ang II.

Given that this is the first comprehensive phenotypic analysis of skeletal muscle obtained from pancreatic cancer patients, we acknowledge that the study has some limitations. First, our study is limited to 20 PDAC patients and 16 non-cancer control subjects and, therefore, our findings should be validated in a larger cohort of patients. Second, although 5% BW loss during 6 months is widely accepted as a diagnostic criterion for cachexia (1) and is the criteria used in the current study, the use of imaging technology can provide a more detailed assessment of skeletal muscle size and changes in skeletal muscle mass over time (17). Third, we did not account for other comorbidities, including concurrent cardiac disorders and insulin resistance, or patient medications, which have the potential to affect cachexia syndrome (50). Despite these limitations, the consistencies in our data across patients within group provide a high level of confidence in our findings.

In summary, our findings demonstrate clinically significant skeletal muscle fibrosis in cachectic PDAC patients that correlates not only with increased BW loss but also with lymph node metastasis and decreased survival. Although future studies are needed to determine the initiating mechanisms leading to muscle fibrosis in response to pancreatic cancer, because we obtained muscle fibers from patients at the beginning of surgery and found similar pathologies in PDAC patients with and without neoadjuvant therapy, we conclude that neither surgery nor therapy can explain the identified pathologies. Based on the findings herein, we speculate that anti-cachexia therapies in PDAC patients may need to include antifibrotic agents in addition to agents that target appetite and protein metabolism.

Funding

This work was supported by the National Institute of Arthritis, Musculoskeletal and Skin Diseases (R01AR060209 to ARJ); the National Cancer Institute (R21CA194118 to ARJ); the UF Health Cancer Center (Bridge Funding to ARJ); the UF Clinical and Translational Science Institute (the UF CTSI is supported by the National Center For Advancing Translational Sciences of the National Institutes of Health [UL1TR001427]; Pilot Award to ARJ); and the V Foundation for Cancer Research (V2015-021 to JGT). RLN is supported by a National Institute of Child Health and Human Development Grant (T32-HD-043730). The Boston University Microarray Core is supported by Clinical and Translational Science Award grant UL1-TR001430.

Notes

Affiliations of authors: Department of Physical Therapy, University of Florida Health Science Center, Gainesville, FL (SMJ, RLN, ARJ); Department of Surgery, College of Medicine, University of Florida Health Science Center, Gainesville, FL (DD, MHG, MEC, JGT).

References

1. Fearon K, Strasser F, Anker SD, et al. Definition and classification of cancer cachexia: an international consensus. *Lancet Oncol*. 2011;12(5):489–495.
2. Evans WJ, Morley JE, Argiles J, et al. Cachexia: a new definition. *Clin Nutr*. 2008;27(6):793–799.
3. Tisdale MJ. Mechanisms of cancer cachexia. *Physiol Rev*. 2009;89(2):381–410.
4. Baracos VE, Martin L, Korc M, et al. Cancer-associated cachexia. *Nat Rev Dis Primers*. 2018;4:17105.
5. Bachmann J, Heiligensetzer M, Krakowski-Roosen H, et al. Cachexia worsens prognosis in patients with resectable pancreatic cancer. *J Gastrointest Surg*. 2008;12(7):1193–1201.
6. Hendifar AE, Chang JI, Huang BZ, et al. Cachexia, and not obesity, prior to pancreatic cancer diagnosis worsens survival and is negated by chemotherapy. *J Gastrointest Oncol*. 2018;9(1):17–23.
7. Delitto D, Judge SM, George TJ Jr, et al. A clinically applicable muscular index predicts long-term survival in resectable pancreatic cancer. *Surgery*. 2017;161(4):930–938.
8. Kahl C, Krahl R, Becker C, et al. Long-term follow-up of the AML97 study for patients aged 60 years and above with acute myeloid leukaemia: a study of the East German Haematology and Oncology Study Group (OSHO). *J Cancer Res Clin Oncol*. 2016;142(1):305–315.
9. Mian OY, Ram AN, Tuli R, et al. Management options in locally advanced pancreatic cancer. *Curr Oncol Rep*. 2014;16(6):388.
10. Vincent A, Herman J, Schulick R, et al. Pancreatic cancer. *Lancet*. 2011;378(9791):607–620.
11. Bockhorn M, Uzunoglu FG, Adham M, et al. Borderline resectable pancreatic cancer: a consensus statement by the International Study Group of Pancreatic Surgery (ISGPS). *Surgery*. 2014;155(6):977–988.
12. Zhou X, Wang JL, Lu J, et al. Reversal of cancer cachexia and muscle wasting by ActRIIB antagonism leads to prolonged survival. *Cell*. 2010;142(4):531–543.
13. Cai D, Frantz JD, Tawa NE Jr, et al. IKKbeta/NF-kappaB activation causes severe muscle wasting in mice. *Cell*. 2004;119(2):285–298.
14. Fearon KC, Glass DJ, Guttridge DC. Cancer cachexia: mediators, signaling, and metabolic pathways. *Cell Metab*. 2012;16(2):153–166.
15. Penna F, Ballaro R, Beltra M, et al. Modulating metabolism to improve cancer-induced muscle wasting. *Oxid Med Cell Longev*. 2018;2018:7153610.
16. Garcia JM, Boccia RV, Graham CD, et al. Anamorelin for patients with cancer cachexia: an integrated analysis of two phase 2, randomised, placebo-controlled, double-blind trials. *Lancet Oncol*. 2015;16(1):108–116.
17. Martin L, Birdsell L, Macdonald N, et al. Cancer cachexia in the age of obesity: skeletal muscle depletion is a powerful prognostic factor, independent of body mass index. *J Clin Oncol*. 2013;31(12):1539–1547.
18. Senf SM, Howard TM, Ahn B, et al. Loss of the inducible Hsp70 delays the inflammatory response to skeletal muscle injury and severely impairs muscle regeneration. *PLoS One*. 2013;8(4):e62687.
19. Senf SM, Dodd SL, McClung JM, et al. Hsp70 overexpression inhibits NF-kappaB and Foxo3a transcriptional activities and prevents skeletal muscle atrophy. *FASEB J*. 2008;22(11):3836–3845.
20. Judge SM, Wu CL, Beharry AW, et al. Genome-wide identification of FoxO-dependent gene networks in skeletal muscle during C26 cancer cachexia. *BMC Cancer*. 2014;14:997.
21. Huang da W, Sherman BT, Lempicki RA. Systematic and integrative analysis of large gene lists using DAVID bioinformatics resources. *Nat Protoc*. 2009;4(1):44–57.
22. Huang DW, Sherman BT, Lempicki RA. Bioinformatics enrichment tools: paths toward the comprehensive functional analysis of large gene lists. *Nucleic Acids Res*. 2009;37(1):1–13.
23. Fink DM, Steele MM, Hollingsworth MA. The lymphatic system and pancreatic cancer. *Cancer Lett*. 2016;381(1):217–236.
24. Uezumi A, Ito T, Morikawa D, et al. Fibrosis and adipogenesis originate from a common mesenchymal progenitor in skeletal muscle. *J Cell Sci*. 2011;124(pt 21):3654–3664.
25. Mann CJ, Perdiguero E, Kharraz Y, et al. Aberrant repair and fibrosis development in skeletal muscle. *Skelet Muscle*. 2011;1(1):21.
26. Kharraz Y, Guerra J, Pessina P, et al. Understanding the process of fibrosis in Duchenne muscular dystrophy. *Biomed Res Int*. 2014;2014:965631.
27. Jolly RD, Palmer DN, Dalefield RR. The analytical approach to the nature of lipofuscin (age pigment). *Arch Gerontol Geriatr*. 2002;34(3):205–217.
28. Sulzer D, Mosharov E, Talloczy Z, et al. Neuronal pigmented autophagic vacuoles: lipofuscin, neuromelanin, and ceroid as macroautophagic responses during aging and disease. *J Neurochem*. 2008;106(1):24–36.
29. Balakrishnan KR, Kuruvilla S, Srinivasan A, et al. Images in cardiovascular medicine. Electron microscopic insights into the vascular biology of atherosclerosis: study of coronary endarterectomy specimens. *Circulation*. 2007;115(14):e388–e390.
30. Acharyya S, Butchbach ME, Sahenk Z, et al. Dystrophin glycoprotein complex dysfunction: a regulatory link between muscular dystrophy and cancer cachexia. *Cancer Cell*. 2005;8(5):421–432.

31. He WA, Berardi E, Cardillo VM, et al. NF-kappaB-mediated Pax7 dysregulation in the muscle microenvironment promotes cancer cachexia. *J Clin Invest*. 2013;123(11):4821–4835.
32. Gissel H. The role of Ca2+ in muscle cell damage. *Ann N Y Acad Sci*. 2005;1066: 166–180.
33. Tamilarasan KP, Temmel H, Das SK, et al. Skeletal muscle damage and impaired regeneration due to LPL-mediated lipotoxicity. *Cell Death Dis*. 2012;3:e354.
34. Das SK, Eder S, Schauer S, et al. Adipose triglyceride lipase contributes to cancer-associated cachexia. *Science*. 2011;333(6039):233–238.
35. Carpenter S, Karpati G. Lysosomal storage in human skeletal muscle. *Hum Pathol*. 1986;17(7):683–703.
36. Linhart A, Elliott PM. The heart in Anderson-Fabry disease and other lysosomal storage disorders. *Heart*. 2007;93(4):528–535.
37. MacDonald EM, Cohn RD. TGFbeta signaling: its role in fibrosis formation and myopathies. *Curr Opin Rheumatol*. 2012;24(6):628–634.
38. Mauviel A. Transforming growth factor-beta: a key mediator of fibrosis. *Methods Mol Med*. 2005;117:69–80.
39. Penafuerte CA, Gagnon B, Sirois J, et al. Identification of neutrophil-derived proteases and angiotensin II as biomarkers of cancer cachexia. *Br J Cancer*. 2016;114(6):680–687.
40. Greco SH, Tomkotter L, Vahle AK, et al. TGF-beta blockade reduces mortality and metabolic changes in a validated murine model of pancreatic cancer cachexia. *PLoS One*. 2015;10(7):e0132786.
41. Grotendorst GR. Connective tissue growth factor: a mediator of TGF-beta action on fibroblasts. *Cytokine Growth Factor Rev*. 1997;8(3):171–179.
42. Leask A, Abraham DJ. TGF-beta signaling and the fibrotic response. *FASEB J*. 2004;18(7):816–827.
43. Duncan MR, Frazier KS, Abramson S, et al. Connective tissue growth factor mediates transforming growth factor beta-induced collagen synthesis: down-regulation by cAMP. *FASEB J*. 1999;13(13):1774–1786.
44. Vial C, Zuniga LM, Cabello-Verrugio C, et al. Skeletal muscle cells express the profibrotic cytokine connective tissue growth factor (CTGF/CCN2), which induces their dedifferentiation. *J Cell Physiol*. 2008;215(2):410–421.
45. Morales MG, Cabello-Verrugio C, Santander C, et al. CTGF/CCN-2 overexpression can directly induce features of skeletal muscle dystrophy. *J Pathol*. 2011;225(4):490–501.
46. Morales MG, Gutierrez J, Cabello-Verrugio C, et al. Reducing CTGF/CCN2 slows down mdx muscle dystrophy and improves cell therapy. *Hum Mol Genet*. 2013;22(24):4938–4951.
47. Morales MG, Cabrera D, Cespedes C, et al. Inhibition of the angiotensin-converting enzyme decreases skeletal muscle fibrosis in dystrophic mice by a diminution in the expression and activity of connective tissue growth factor (CTGF/CCN-2). *Cell Tissue Res*. 2013;353(1):173–187.
48. Murphy KT, Chee A, Trieu J, et al. Inhibition of the renin-angiotensin system improves physiological outcomes in mice with mild or severe cancer cachexia. *Int J Cancer*. 2013;133(5):1234–1246.
49. Sanders PM, Russell ST, Tisdale MJ. Angiotensin II directly induces muscle protein catabolism through the ubiquitin-proteasome proteolytic pathway and may play a role in cancer cachexia. *Br J Cancer*. 2005;93(4): 425–434.
50. Kazemi-Bajestani SM, Becher H, Fassbender K, et al. Concurrent evolution of cancer cachexia and heart failure: bilateral effects exist. *J Cachexia Sarcopenia Muscle*. 2014;5(2):95–104.